Article

Nitrate Nitrogen Quantification via Ultraviolet Absorbance: A Case Study in Agricultural and Horticultural Regions in Central China

Yiheng Zang [1,†], Jing Chen [1,†], Muhammad Awais [1], Mukhtar Iderawumi Abdulraheem [1], Moshood Abiodun Yusuff [1], Kuan Geng [1], Yongqi Chen [1], Yani Xiong [1], Linze Li [1], Yanyan Zhang [1], Vijaya Raghavan [2], Jiandong Hu [1,3,*], Junfeng Wu [1] and Guoqing Zhao [4,*]

1   Henan International Joint Laboratory of Laser Technology in Agriculture Sciences, College of Mechanical & Electrical Engineering, Henan Agricultural University, Zhengzhou 450002, China; yheng@stu.henau.edu.cn (Y.Z.); jingchen@henau.edu.cn (J.C.); dr.muhammad.awais@henau.edu.cn (M.A.); abdulraheem@stu.henau.edu.cn (M.I.A.); yusufbinmasud01@stu.henau.edu.cn (M.A.Y.); gengkuan@stu.henau.edu.cn (K.G.); cyq@stu.henau.edu.cn (Y.C.); xiongyani@stu.henau.edu.cn (Y.X.); lilinze@henau.edu.cn (L.L.); zyanyan0923@henau.edu.cn (Y.Z.); jfwu@henau.edu.cn (J.W.)
2   Department of Bioresource Engineering, Faculty of Agriculture and Environmental Studies, McGill University, Sainte-Anne-de-Bellevue, QC H9X 3V9, Canada; vijaya.raghavan@mcgill.ca
3   State Key Laboratory of Wheat and Maize Crop Science, Zhengzhou 450002, China
4   School of Management, Swansea University, Swansea SA2 8PP, UK
*   Correspondence: jdhu@henau.edu.cn (J.H.); guoqing.zhao@swansea.ac.uk (G.Z.)
†   These authors contributed equally to this work.

Abstract: Soil nitrate nitrogen (NO_3^--N) is a key indicator of agricultural non-point source pollution. The ultraviolet (UV) dual-wavelength method is widely used for NO_3^--N detection, but interference from complex soil organic matter affects its accuracy. This study investigated how organic matter influences NO_3^--N detection by optimizing UV dual-wavelength combinations. Density functional theory (DFT) calculations showed slight spectral broadening of fulvic and humic acids in the presence of NO_3^--N under UV spectrum. Standard solutions and soil samples were used to compare the detection performance of different wavelength pairs. The findings indicated that the dual-wavelength combination of 235 nm/275 nm is optimal rather than 220 nm/275 nm for measuring soil samples at NO_3^--N concentrations exceeding 5 mg·L^{-1}. The 235/275 nm method gave an average calibration coefficient of 1.57. Compared to the national standard and flow analysis methods, the average relative errors were 19.7% and 22.3% ($p < 0.001$), respectively, indicating its suitability for practical soil applications. These results demonstrate the method's potential for rapid and accurate NO_3^--N detection in real soil samples, supporting its application in environmental monitoring and agricultural management.

Keywords: nitrate nitrogen in soil; ultraviolet dual-wavelength; agricultural non-point source pollution (ANPS); soil organic matter; calibration coefficient

1. Introduction

Growing concerns about the environmental impact of excessive fertilizer use, particularly excess nutrient deposits in soils, and understanding NO_3^--N levels have become critical to sustainable agricultural practices [1,2]. Elevated NO_3^--N concentrations present a significant risk to the ecological environment, potentially resulting in groundwater contamination and eutrophication, which can adversely affect soil, water quality, and

human health [3,4]. However, due to its high solubility and fluidity in water, NO_3^--N is easily biodegraded, so its measurement results are easily interfered with by many environmental factors.

For example, changes in frequency and mode of farmland irrigation will affect the migration and transformation of NO_3^--N in soil [5,6]. The key factor that influences measurement accuracy is the content of soil organic matter (SOM), which plays an important role in the storage and stability of NO_3^--N by reacting with or adsorbing NO_3^--N ions [7,8]. Overlapping spectral absorption from NO_3^--N and organic matter can result in substantial measurement errors when employing the Ultraviolet (UV) dual-wavelength method. Numerous studies have illustrated the intricacy of this relationship, underscoring the necessity for calibration methods that consider SOM variations to enhance the accuracy of NO_3^--N measurements in the field [9,10]. Therefore, considering the impact of organic matter in NO_3^--N measurements is crucial to ensure accuracy, especially in soils with high organic content [11,12].

Traditionally, the determination of NO_3^--N in soil mainly depended on laboratory methods, such as the ion-selective electrode method, ion chromatography, which commonly requires the use of chemical reagents to accurately determine the concentration of NO_3^--N in soil [13,14]. Thus, these laboratory methods, while excellent in accuracy, are cumbersome, time-consuming, and not cost-effective. On the other hand, dangerous chemical reagents, such as strong acids and alkali, used in experiments not only have high technical requirements for operators but also pose certain safety risks [15]. In modern agricultural practices, precision agriculture technology has gradually become an important measure to improve crop productivity by helping farmers recommend fertilizer more rationally, and reduce environmental pollution through real-time monitoring of soil nutrient status [16,17]. Nonetheless, traditional laboratory methods struggle to fulfill this demand as they are unable to rapidly deliver soil data on site. This delay may result in excessive fertilization or the failure to apply fertilizers at the ideal time, subsequently impacting crop yields and the health of the environment [18,19].

In recent years, sensor-based real-time monitoring technology has gradually emerged as a possible alternative, such as spectral analysis, electrochemical sensors, and the Internet of Things, which can make rapid and non-destructive determination of NO_3^--N in soil [20–22]. These approaches not only improve inspection efficiency but also enable remote monitoring and decision making through data networking, providing timely and reliable data support for agricultural management [23,24]. Through the application of precise resource allocation and an intelligent management system, the efficiency of agricultural production factors has been significantly improved, and agricultural errors have been reduced [25].

Ultraviolet spectroscopy is currently very popular for detecting soil NO_3^--N as a promising alternative to traditional chemical analysis [11]. In particular, the ultraviolet dual-wavelength method has shown great potential in overcoming the interference caused by SOM on NO_3^--N measurements [26,27]. The method includes measuring the ultraviolet light absorption of different substances at specific wavelengths, one is sensitive to NO_3^--N and organic matter (220–240 nm), and the other is sensitive to organic matter only (254–280 nm). By quantifying the difference in absorbance at two specific wavelengths, the concentration of the target sample can be accurately determined from a mixture with potentially interfering components [28–30]. In addition, the dual ultraviolet wavelength combination is also a key factor in the determination of the calibration coefficient. Eight soil types in different ecological regions of Inner Mongolia were selected to determine NO_3^--N in soil, and the influence of wavelength selection and soil type on the calibration coefficient of ultraviolet spectrophotometry was investigated [31].

Although the NO_3^--N measurement instrument has made important advances with ultraviolet spectrophotometry in the measurement of NO_3^--N in soil [32], the complexity of relying on broadband ultraviolet spectrophotometers and bulky deuterium lamps as ultraviolet light sources makes the technology not yet suitable for commercial applications. With the breakthrough of AlGaN semiconductor materials with a wide bandgap [33], deep ultraviolet light-emitting diodes (UVC-LEDs) with an operating band of 235–290 nm have made a breakthrough in optical power output performance [34,35]. This progress not only promotes the technological innovation of the miniaturized spectrophotometric nitrate sensor, but also systematically improves the core performance of the sensor through the collaborative optimization and precision structural design of LEDs and photodiodes (PDs)—while increasing the sensitivity by 20% and extending the linear detection range to 0–20 mg·L^{-1}, where long-term operational stability is achieved [36]. At present, it has been successfully applied to a water quality online monitoring system, providing intelligent solutions with high precision and low power consumption for the environmental monitoring field [37,38].

This study primarily focuses on examining the impact of NO_3^--N measurements in soil that varies in organic matter content. The assessment of NO_3^--N in soil using UV dual-wavelength combinations of 220 nm/275 nm and 235 nm/275 nm will be investigated with soil samples from agricultural and horticultural regions, China. The impact of NO_3^--N in soil with varying organic matter contents on the calibration coefficient α of the ultraviolet dual-wavelength method is examined, followed by further optimization. The ultimate objective of this research is to create a more dependable and efficient method for measuring NO_3^--N in the field, which will have substantial advantages for environmental monitoring and precision agriculture.

2. Materials and Methods

2.1. Study Area and Field Sampling

The samples originated from agricultural and horticultural regions in Henan province, a significant agricultural hub in central China recognized for its extensive crop cultivation (Figure 1a,b). These regions have been meticulously chosen to yield a representative sample of agricultural methodologies and crop varieties. In this experiment, different soil samples were collected from the Mengzhou Kiwifruit planting zone (112°47′31.5″ E, 34°54′23.5″ N) in Jiaozuo and the Yichuan Wheat planting zone (112°25′30.4″ E, 34°25′31.1″ N) in Luoyang. The sampling points in the Yichuan area were random (Figure 1c), and the kiwifruit planting zone was divided into 10 sample areas (Figure 1d). The plum blossom point method [39] was used to collect three soil samples ranging in depth from 0 to 30 cm in each plot.

2.2. Chemical Treatment and Analysis

In this study, standard NO_3^--N solutions (0–25.0 mg·L^{-1}) were prepared using analytical-grade NaNO$_3$ (purity ≥ 99%, Sinopharm Group, Beijing, China) and deionized water. Potassium chloride (KCl, purity 99.5%, Sinopharm Group, Beijing, China) was used for soil extraction. Absorbance at 220 nm, 235 nm, and 275 nm was recorded using a UV–visible spectrophotometer (Nanjing Feller Instrument Co., Ltd, Nanjing, China) and a self-developed integrated flow injection analyzer (IRFA) to establish calibration curves.

To assess the effects of organic matter, humic acid (HA, 104 mg·L^{-1}) and fulvic acid (FA, 63 mg·L^{-1}) solutions were added to the NO_3^--N standards, and calibration coefficients (220/275 nm and 235/275 nm absorbance ratios) were calculated.

Additionally, 24 soil samples were collected from kiwifruit and wheat plantations. After extraction with 100 mL of 1 M KCl for 1 h, the mixtures were filtered to obtain soil extracts. To assess the impact of varying organic matter content on the selection of

the optimal detection wavelength combination for NO_3^--N, 10 samples of soil from two regions were divided into multiple aliquots and processed as described. To simulate a range of NO_3^--N concentrations, mixed extracts were spiked with known volumes of 1 g·L^{-1} NO_3^--N standard solution and KCl, forming 7–9 concentration gradients. The final volume of each solution was adjusted to 50 mL. Dual-wavelength absorbance measurements at 220/275 nm and 235/275 nm were then performed to evaluate detection accuracy.
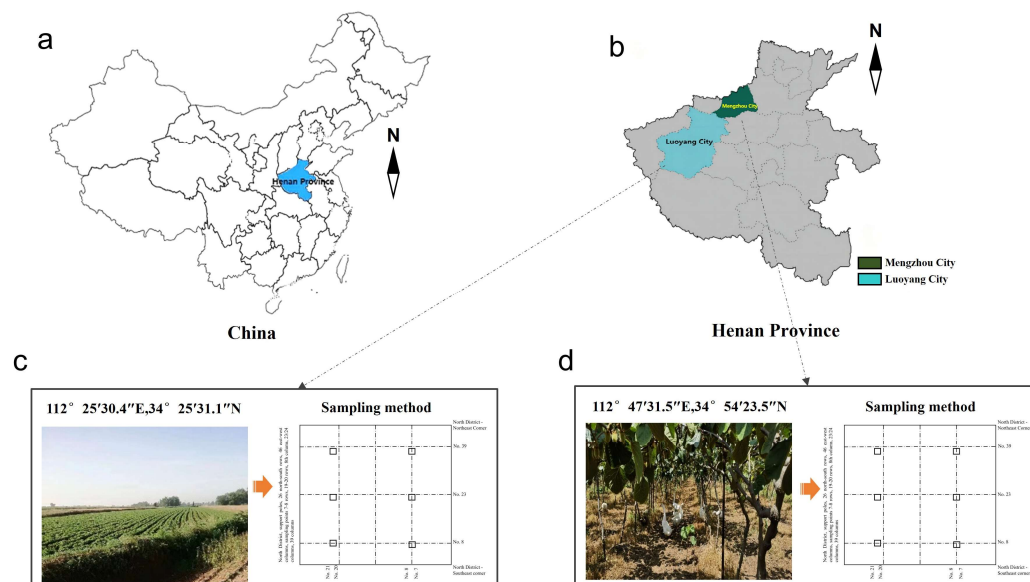

Figure 1. The marked study areas. Map of China (**a**) and Henan province (**b**); The photos of the sampling locations in Yichuan (**c**) and Mengzhou (**d**).

2.3. Absorption Spectrum Computation of Organic Matter and NO_3^-

Fulvic acid (FA) and humic acid (HA) are the main components of soil organic matter [40,41]. HA, a major fraction of humic substances, is widely present in soil, water, and sediments [42], while FA plays a key role in the humus structure of nutrient-rich soils and regulates plant growth. The presence of organic matter can interfere with the accurate determination of soil NO_3^--N concentrations [43].

To investigate the absorption spectrum of these two organic matters and NO_3^--N, density functional theory (DFT) calculations were conducted using Gaussian 16 ab initio software [44]. Structural optimizations of fulvic acid, humic acid, and NO_3^--N were performed at the M06-2X/def2-TZVP theoretical level. Frequency calculations were conducted on the optimized molecules to verify that the optimized structures represent the minima on the potential energy surface. Based on the calculations, the electrostatic potential (ESP) of the pertinent molecule or ion was exported using Multiwfn software [45] and visualized with VMD software [46]. As illustrated in Figure 2, NO_3^- is enveloped by a robust electronegative electric field, attributable to the presence of three oxygen atoms (Figure 2a). An electro-positive electric field is present in the vicinity of the surfaces of HA and FA (Figure 2b,c). Consequently, NO_3^- is eventually trapped or bound by organic matter to a certain degree by electrostatic interaction. The binding free energies, ΔG_{bind} of NO_3^- with FA or HA, are -8.57 kcal·mol^{-1} and -6.95 kcal·mol^{-1}, respectively (Figure 2d,e), indicating a relatively strong electrostatic interaction between the organic compound and NO_3^-. The measurement of NO_3^- is readily affected by organic matter. The binding free energy ΔG_{bind} was computed with the following Equation (1):

$$\Delta G_{bind} = G_{FA/HA+NO3^-} - G_{FA/HA} - G_{NO3^-} \tag{1}$$

where the $G_{FA/HA+NO3^-}$ denotes the Gibb's free energy of the complex, namely, the association of the FA/HA molecule with the nitrate ion, $G_{FA/HA}$ signifies the Gibb's free energy of the unbound FA/HA molecule, and G_{NO3^-} indicates the Gibb's free energy of the free NO_3^--N. The values on the right side of Equation (1) were derived using the corresponding frequency computations.
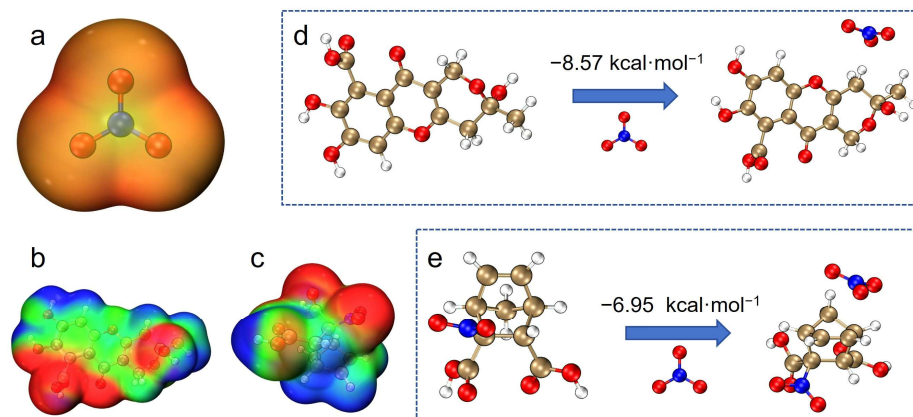

Figure 2. The electrostatic potential (ESP) of (**a**) NO_3^-, (**b**) FA molecule, and (**c**) HA molecule. (**d,e**) show the binding energy calculations of NO_3^--N with (**b**) FA and (**c**) HA. In these pictures of ESP, the red color represents the electronegativity, the blue color represents the electropositivity, and the green color represents the electroneutrality.

The calculated UV spectra of the relevant molecules or ions in aqueous solution were obtained using the time-dependent density functional theory (TDDFT) method, using the optimized structures at the M06-2X/6-311+G (2 d,p) theoretical level. The SMD implicit solvent model was used to replicate the aqueous environment in order to theoretically support the impact of organic matter on the absorption spectrum of NO_3^--N (Figure 3). There exists a significant overlap between NO_3^--N and organic matters at the wavelength below 225 nm, particularly for NO_3^--N and HA, which complicates the measurement of NO_3^--N in the mixed solution system when relying on adsorption at a single wavelength. Furthermore, the amalgamation of NO_3^--N with organic matters solely exhibits the adsorption properties of the latter, hence diminishing the measurability of NO_3^--N. Fortunately, the adsorption intensity of organic matters varies significantly upon combination, particularly for HA, enabling measurement of NO_3^--N by an indirect method, such as dual wavelengths.
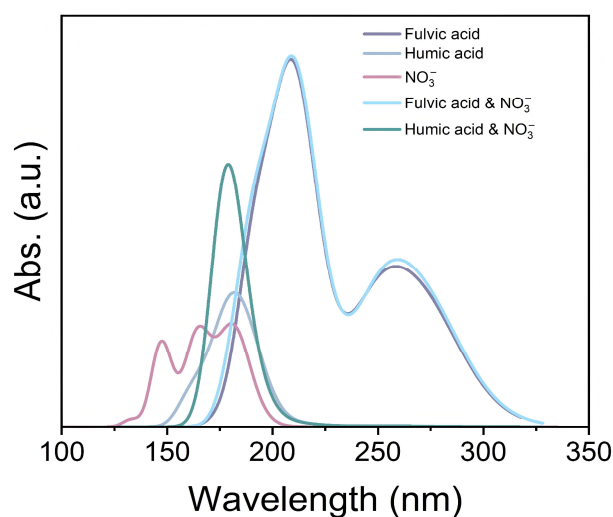

Figure 3. Calculated UV spectra of FA, HA, and NO_3^--N and their combination.

2.4. NO_3^--N Measurement System Using Dual-Ultraviolet Wavelength Absorption

The research indicated that NO_3^--N in soil exhibits a strong absorption near 220 nm, but no absorption characteristics at 275 nm [47]. The direct measurement of the NO_3^--N concentration in soil samples is significantly restricted by the extensive interference of soil organic matter in the dual-ultraviolet wavelength absorption. Here, a key calibration coefficient α, the dual-wavelength spectral absorption ratio of organic matter in the soil solution, the measured A_{275} is multiplied by this coefficient α and then reduced by A_{220} to eliminate the interference. However, the composition of soil organic matter is highly diverse and complex, which complicates its spectral characteristics [48]. As a result, it is difficult to directly and accurately determine the calibration coefficient α through theoretical calculation.

Therefore, for the different soil types or the same soil type with different soil organic matter content, the calibration coefficient α should be improved before the measurement. In this work, experiments were carried out for soil types with different organic matter and NO_3^--N concentration, and the calculation formula of NO_3^--N concentration is shown in Equation (2):

$$C_{NO3^--N} = k \times (A_{220,235} - \alpha \times A_{275}) + b \qquad (2)$$

where C_{NO3^--N} is the concentration of NO_3^--N in the sample solution; k is the conversion coefficient, which is used to convert the corrected absorbance into the concentration of NO_3^--N; $A_{220,235}$ is one of the absorbances at 220 nm and 235 nm; α is the calibration coefficient, which is derived from the absorbance ratio of multiple sets of organic matter at 220 nm or 235 nm to 275 nm; and b is the error used to compensate for systematic errors or background signals in the experiment.

2.5. Statistical Analysis

All statistical analyses, including linear regression fitting and calculation of the determination coefficients (R^2), were performed using Origin 2022 (OriginLab Corporation, Northampton, MA, USA) based on the least square method. To evaluate the significance of the regression models, *p*-values were calculated by Origin 2022. Specifically, the overall significance of each linear regression was assessed using an F-test, and the associated *p*-values (Prob > F) were reported. Graphs were also generated using Origin 2022.

3. Results

3.1. Absorbance of NO_3^--N Solutions at 220 nm,235 nm, and 275 nm

The absorbance analysis curve shown in Figure 4 illustrates the characteristics of the ultraviolet wavelength method for determining NO_3^--N concentrations. Within the low concentration range of 0–5 mg·L^{-1}, the absorbance at 220 nm increases sharply with NO_3^--N concentration, indicating that this wavelength is particularly sensitive to NO_3^--N in this interval. The high determination coefficient ($R^2 = 0.9983$, $p < 0.001$) supports its reliability for detecting low concentrations of NO_3^--N. For concentrations between 0 and 20 mg·L^{-1}, absorbance at 235 nm shows minimal variation but maintains a notable linear relationship with a determination coefficient (R^2) of 0.9978 ($p < 0.001$). This makes 235 nm a preferable wavelength for quantifying higher levels of NO_3^--N, especially when avoiding saturation effects at lower wavelengths. In contrast, absorbance at 275 nm exhibits a relatively small linear slope, consistent with its role as a background correction wavelength.
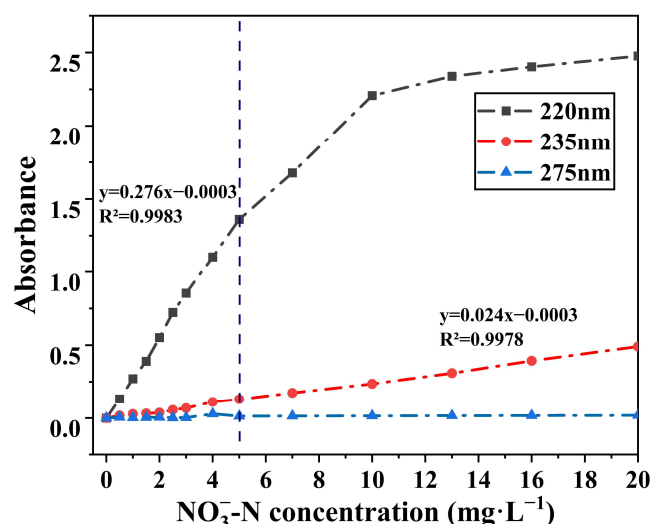
Figure 4. Absorbance of different NO_3^--N concentrations at 220 nm, 235 nm, and 275 nm wavelengths.

3.2. Analysis of Calibration Coefficients on Samples with Organic Matter

Preliminary experimental results indicate that for FA samples of varying concentrations, absorbance exhibits an increasing trend at several wavelengths (220 nm, 235 nm, 275 nm) as concentration rises (Figure 5). The rate of rise in absorbance at 220 nm is notably rapid, suggesting that within the examined concentration range, the sensitivity of the 220 nm wavelength to FA is elevated (Figure 5a). Like FA, the absorbance of HA likewise escalates with concentration across all wavelengths. In addition, the absorbance ratio of FA and HA (220 nm/275 nm and 235 nm/275 nm, denoted as calibration coefficient α) exhibits considerable variability in the low concentration range (0~5 mg·L^{-1}) (Figure 5c,d). In comparison with the 220 nm/275 nm wavelength combination, the 235 nm/275 nm wavelength combination exhibits a more gradual variation in the absorbance ratio of FA and HA. At low concentrations, the variation in absorbance ratio was less pronounced, while at medium and high concentrations, the absorbance ratio changed smoothly and linearly between 0.95 and 1.31.

3.3. Experiment and Analysis of NO_3^--N in the Samples with Adding Organic Matters

Figure 6 presents the absorbance values and corresponding absorbance ratios at 220 nm, 235 nm, and 275 nm after the addition of two types of organic matter.

The influence of NO_3^--N concentration on the calibration coefficients remains relatively stable across the tested wavelengths (220 nm and 235 nm) (Figure 6a,b). When fulvic acid (FA) was added, the calibration coefficient (absorbance ratio) at 220 nm/275 nm ranged from 2.2 to 3.1, while the ratio at 235 nm/275 nm varied from 1.4 to 2.0, indicating a narrower fluctuation at the latter wavelength combination (Figure 6c). Upon the addition of humic acid (HA), the calibration coefficients showed even smaller variations: 1.15–1.26 for 220 nm/275 nm and 1.09–1.19 for 235 nm/275 nm (Figure 6d).
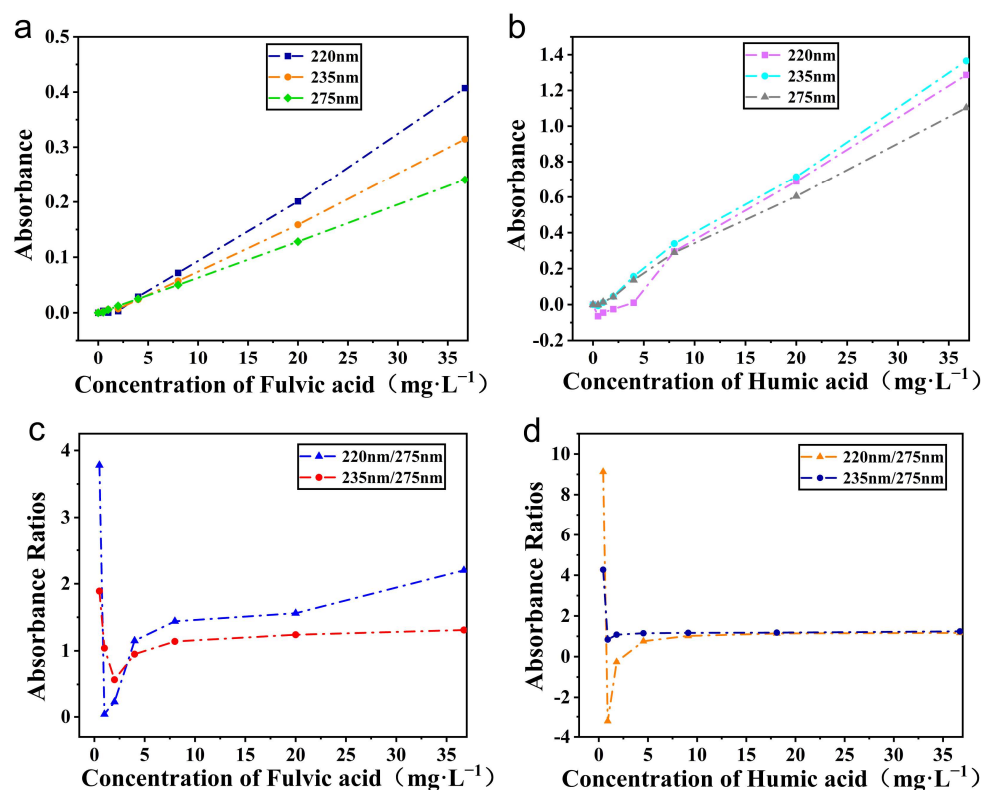
Figure 5. The absorbance of the standard solutions of (**a**) fulvic acid and (**b**) humic acid at the wavelengths of 220 nm, 235 nm, and 275 nm; The absorbance ratios (220/275 and 235/275) of the standard solutions of (**c**) fulvic acid and (**d**) humic acid.
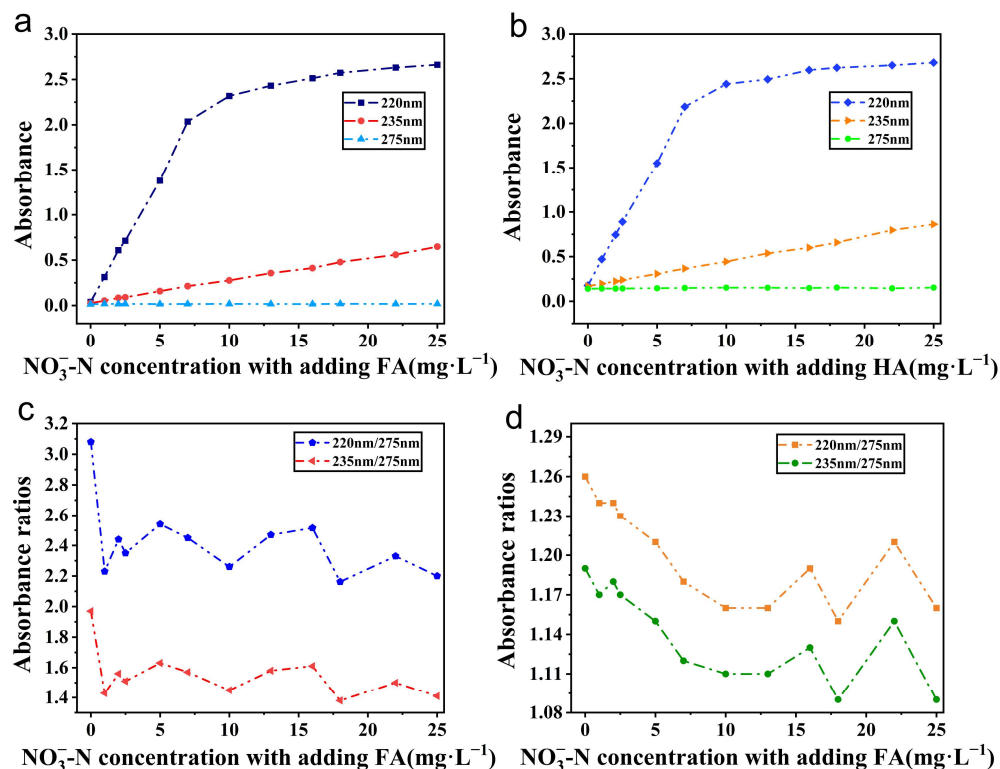

Figure 6. The absorbance of the NO_3^--N standard solutions with (**a**) adding FA and (**b**) HA at the wavelengths of 220 nm, 235 nm, and 275 nm; The absorbance ratios (220/275 and 235/275) of the NO_3^--N standard solutions with adding (**c**) FA and (**d**) HA.

3.4. Experiments for Actual Soil Samples

In this experiment, a total of 18 soil samples were gathered from both the northern and southern regions of the kiwifruit planting base located in Mengzhou City, Henan Province. Additionally, 6 soil samples were collected from the Yichuan wheat planting area in Luoyang City. To ensure soil fertility and promote the healthy growth of kiwifruit or other crops, the experimental study outlined above was validated, and the actual concentrations of soil NO_3^--N and organic matter content were assessed.

As shown in Figure 7, soil samples measured at this time have a noticeable range in organic matter concentrations and NO_3^--N concentrations. The organic matter concentrations of kiwifruit plantation range from 15.18 to 24.03 g·kg^{-1}, while those of Yichuan wheat plantation range from 3.33 to 5.29 g·kg^{-1} (Figure 7a). The NO_3^--N concentrations of kiwifruit plantation range from 3.12 to 28.29 mg·kg^{-1}, while those of Yichuan wheat plantation range from 0.91 to 4.68 mg·kg^{-1} (Figure 7b).
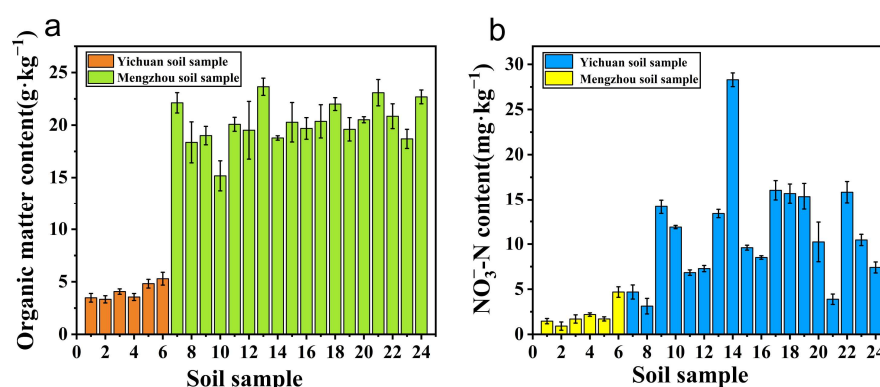

Figure 7. Measured (**a**) organic matter content and (**b**) NO_3^--N content in Yichuan wheat planting and horticultural kiwifruit fields.

The measured NO_3^--N concentrations (obtained via instrument calibration) were compared with the theoretical values calculated using Equation (3). The resulting detection errors under the 220/275 nm and 235/275 nm wavelength combinations were analyzed to assess the applicability and reliability of each dual-wavelength approach.

$$C_1 \times V_1 = C_2 \times V_2 \tag{3}$$

where C_1 and V_1 are the concentration and volume of the initial solution. C_2 and V_2 are the concentration and volume after dilution or concentration.

The organic matter content in the soil of the kiwi cultivation region in Mengzhou is comparatively elevated. At low NO_3^--N concentrations (<4.8 mg·L^{-1}), the discrepancy between the calculated and theoretical concentrations for the two wavelength combinations is minimal. However, as the NO_3^--N concentration rises (>4.8 mg·L^{-1}), the variance in detection results between the 220 nm/275 nm wavelength combination becomes pronounced (Figure 8a). The Yichuan agricultural planting area exhibits a relatively low soil organic matter content, with no variation in detection results between the 220 nm and 235 nm wavelengths, particularly at low concentrations (<6 mg·L^{-1}). Nonetheless, at elevated concentrations, the 235 nm/275 nm wavelength combination exhibits a relative detection advantage (Figure 8b).
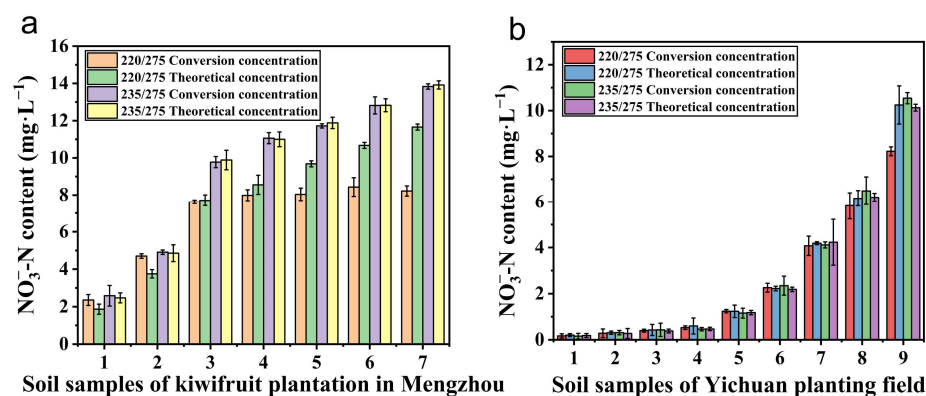
Figure 8. Measured NO_3^--N content in (**a**) Mengzhou kiwifruit planting zone, (**b**) Yichuan wheat planting field.

To further validate the reliability of the 235 nm/275 nm dual-wavelength method for determining soil NO_3^--N using a calibration coefficient of 1.57, a comparative analysis was performed against the widely used flow injection analysis method and the national standard dual-wavelength method (calibration coefficient $\alpha = 2.23$) (Figure 9a,b). The NO_3^--N concentrations measured by the three methods exhibited strong linear relationships. The determination coefficients (R^2) between the proposed method and the flow analysis method, and between the proposed method and the national standard method, were 0.962 and 0.961, respectively, with both comparisons yielding statistically significant correlations ($p < 0.001$).
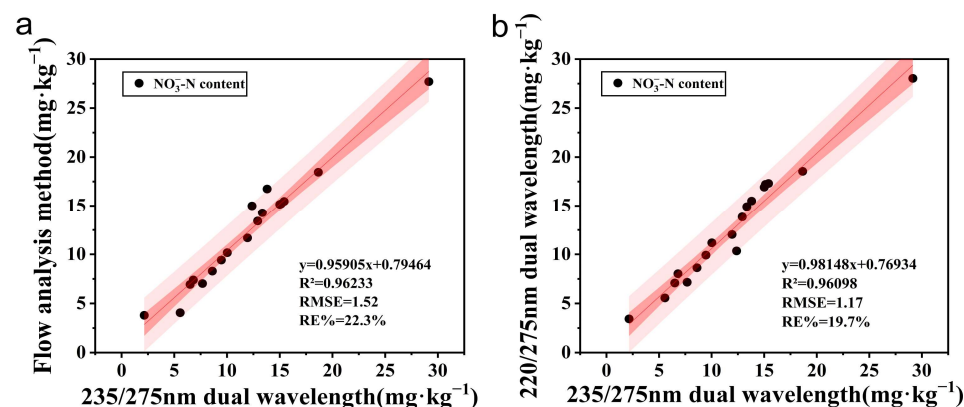

Figure 9. Correlation of NO_3^--N content measured by 235 nm/275 nm method and other different methods, such as (**a**) flow analysis method, (**b**) Chinese national standard dual-wavelength method (220 nm/275 nm).

4. Discussion

4.1. Influence of Different Concentrations of NO_3^--N on Its Dual-Wavelength Determination

As shown in Figure 4, within a specific concentration range, both 220 nm and 235 nm wavelengths demonstrate excellent linear correlation with NO_3^--N absorption, demonstrating strong potential for dual-wavelength UV spectrophotometric analysis. The absorbance at 220 nm is notably high due to the strong molar absorptivity of NO_3^--N, making it highly sensitive for low-concentration detection. This observation is consistent with previous studies, which also identified 220 nm as the optimal wavelength for detecting trace levels of nitrate in aqueous solutions [49,50].

However, when the NO_3^--N concentration exceeds approximately 5 mg·L^{-1}, the absorbance at 220 nm nears saturation (about 2.5 absorbance units), exhibiting non-linear behavior. This saturation effect has been reported in similar studies and is attributed to

limitations in the optical system such as stray light interference and detector overload [49]. In contrast, the absorbance at a wavelength of 235 nm exhibits a more stable and linear response across a broader concentration range. Prior research has highlighted the suitability of 235 nm for medium to high NO_3^--N concentrations, where 220 nm becomes unreliable or necessitates tedious dilution steps [51].

Our results corroborate this finding, as the absorbance analysis demonstrates a sensitivity of 220 nm for low concentrations, a linear behavior of 235 nm for higher concentrations, and a function of 275 nm as a background correction wavelength. For concentrations exceeding 5 mg·L^{-1}, 235 nm provides a more reliable and efficient alternative, especially when organic interferences are minimal or absent. These findings not only align with previous work but also contribute a practical threshold (~5 mg·L^{-1}) for wavelength switching between 220 nm and 235 nm. Unlike earlier studies that typically focused on fixed-wavelength calibration [52], our research proposes a concentration-dependent wavelength selection strategy.

4.2. The Influence of Different Organic Matter on Its Dual-Wavelength Calibration Coefficient

For the difference in absorbance, HA possesses a more intricate molecular structure, an elevated molecular weight, and more functional groups that can absorb ultraviolet light [53]. These variables also lead to HA exhibiting greater absorbance values in the UV region than FA (Figure 5b). Moreover, within the tested range, variations in organic matter concentration significantly influence the absorbance ratio (Figure 5c,d). The consistent and linear response at medium-to-high concentrations suggests that the 235 nm/275 nm wavelength combination is more suitable for quantitative detection under these conditions.

Given the variability of organic matter composition in soils, particularly the fluctuating HA/FA ratios, stable calibration becomes critical [54,55]. The 235 nm/275 nm wavelength combination demonstrates a more consistent calibration coefficient ($\alpha \approx 1.57$) across different organic matter types and concentrations, compared to the standard 220 nm/275 nm ratio ($\alpha = 2.23$, per GB/T 32737-2016 [56]) and a more stable trend, thereby more effectively fulfilling the measurement requirements for NO_3^--N in soil. In addition, the calculation formula of calibrated NO_3^--N concentration is shown in Equation (4):

$$C_{NO3^--N} = k \times (A_{235} - 1.57 \times A_{275}) + b \qquad (4)$$

where $A_{235} - 1.57 \times A_{275}$ is the calibrated absorbance. k is the conversion coefficient, which is used to convert the calibrated absorbance into the concentration of NO_3^--N.

As shown in Figure 6a,b, the presence of HA and FA significantly increases absorbance values at both 220 nm and 235 nm, confirming that organic matter interferes with NO_3^--N detection. However, at higher NO_3^--N concentrations (>5 mg·L^{-1}), the absorbance at 235 nm remains more stable, reducing risks of saturation or signal distortion. Similar results were reported by Dong et al., who found that longer UV wavelengths can effectively suppress the matrix effect of dissolved organic matter during nitrate analysis [57]. In summary, the 235 nm/275 nm combination offers enhanced robustness for NO_3^--N determination in complex soil extracts, especially when organic interference is significant. Thus, it is more suitable for stable NO_3^--N quantification in the presence of humic substances. This finding supports a practical, concentration, and matrix-informed wavelength selection strategy.

4.3. Influence of NO_3^--N Determination in Actual Soil and Applicability of Wavelength

Determination of actual soil, when we validated the 235/275 nm dual-wavelength combination for soil NO_3^--N measurement, effectively mitigates the impact of higher content of organic matter on the measurement results. Considering that the organic matter content in typical agricultural soils was from 1% to 6%, while wetland or horticultural regions

may have organic matter concentrations as high as 20% or more [58,59], the determination results need to be optimized for different soil types and terrain.

This study focused on crop-growing areas in the central region of China, including various soil types and organic matter content, to support more accurate NO_3^--N monitoring strategies for regional soil management. To further explore the application effect of the dual-wavelength combination on the actual soil measurement, we mixed the soil extract and re-measured the standard. Initial investigations suggest that the organic matter content influences the precise measurement of NO_3^--N levels in soil (Figure 8a,b). In instances of low organic matter content (Yichuan soil sample), the influence of wavelength on detection outcomes is more contingent upon the actual NO_3^--N concentrations. The variance in detection results is minimal when employing the 220 nm/275 nm dual wavelength for measuring low concentrations of NO_3^--N, whereas the 235 nm/275 nm dual wavelength can precisely ascertain the NO_3^--N content in soil at 10 mg·L^{-1}. Nevertheless, for solutions with elevated organic matter content (Mengzhou soil sample), the increase in NO_3^--N concentration amplifies the influence of wavelength on detection outcomes. The 220 nm/275 nm dual wavelength is unable to correctly measure 4.8 mg·L^{-1} of NO_3^--N, likely due to UV saturation or spectral overlap with dissolved organics [60,61]. Consequently, the 235 nm/275 nm dual-wavelength combination is more suitable.

Moreover, the NO_3^--N content measured by the dual-wavelength method of 235 nm/275 nm was highly correlated with the national standard method, and the relative error was also low. Comparing the flow analysis method and the national standard dual-wavelength method, the root-mean-square error range is 1.52~1.17, and the average relative error range is 19.7%~22.3%. These results demonstrate the method's accuracy and field relevance. To further reduce the relative error and achieve rapid detection, UV-based sensor systems with fixed optical paths and UVLED sources can improve detection stability and minimize interference. Figure 10 illustrates the soil NO_3^--N measurement system based on dual-ultraviolet wavelength absorption (235 nm and 275 nm UVLED). The system uses two wide-bandgap semiconductor UV photodiodes for real-time online monitoring of NO_3^--N. After photoelectric conversion and signal amplification, the signals are transmitted to a microcontroller for processing. When combined with soil-specific calibration models, such sensors offer better accuracy and are more suitable for in-field NO_3^--N monitoring [62,63].
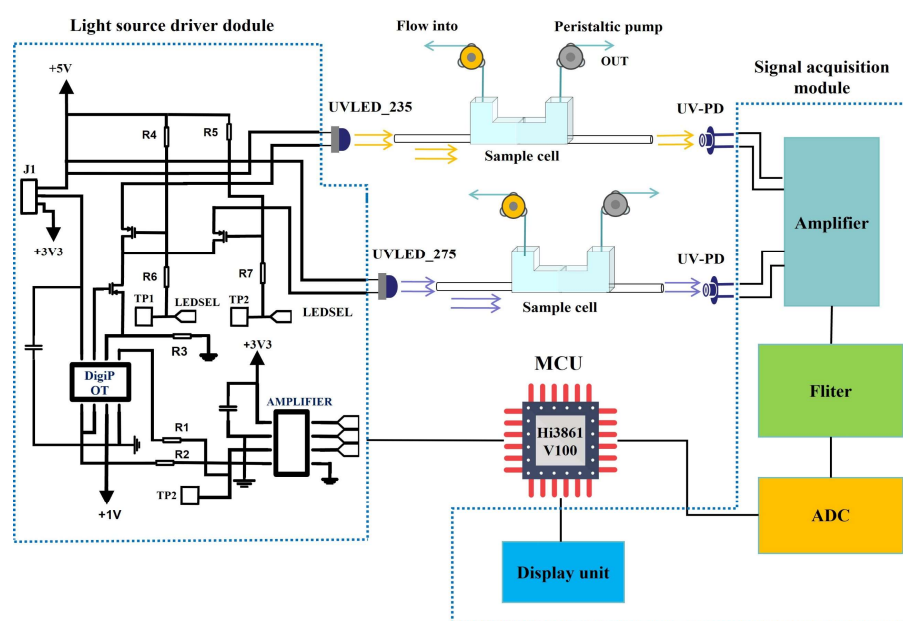

Figure 10. Schematic diagram of NO_3^--N determination by ultraviolet dual-wavelength method based on UVLED.

Overall, this study provides a foundation for improving NO_3^--N detection accuracy under varying SOM conditions. In addition, it is also important to recognize that external environmental and management factors—such as crop cultivation patterns, climate variability, and organic farming practices—can considerably influence the distribution and dynamics of soil NO_3^--N, fulvic acid (FA), and humic acid (HA), especially within the top 30 cm of soil [64,65]. Different crops vary in their nitrogen uptake and root exudation profiles, which affect nitrate mobility and organic matter transformation [66]. In addition, organic farming practices—such as compost application, reduced synthetic fertilizer input, and cover cropping—can significantly increase soil organic carbon and microbial activity, leading to changes in the composition and reactivity of humic substances [67,68]. While these factors were not directly examined in this study, they represent critical areas for future research, which could help refine nitrate detection methods by accounting for variable environmental and biological influences.

5. Conclusions

This study confirms that UV dual-wavelength detection methods, particularly the 235 nm/275 nm combination, are more reliable for quantifying soil NO_3^--N in the presence of organic matter. The influence of organic components was validated through both DFT simulations and laboratory experiments, revealing their impact on UV absorbance and the need for calibration. By introducing an optimized calibration coefficient, the method effectively reduces matrix interference and enhances measurement accuracy. Compared to conventional techniques, it offers a simplified approach with reduced reagent use and improved measurement reliability. While the current results are based on selected soil types from specific agricultural regions, further validation across broader soil conditions is necessary. Overall, this UV dual-wavelength approach holds strong potential for supporting environmental monitoring, precision fertilization, and routine soil testing in agriculture.

Author Contributions: Y.Z. (Yiheng Zang): Writing—review & editing, Writing—original draft, Investigation, Methodology. J.C.: Writing—review & editing, Writing—original draft, Validation. M.A.: Writing—review & editing, Investigation. M.A.Y.: Writing—review & editing. K.G.: Data curation. Y.C.: Software. Y.X.: Formal analysis. L.L.: Resources. Y.Z. (Yanyan Zhang): Investigation. M.I.A.: Validation. V.R.: Visualization. J.H.: Writing—review & editing, Supervision, Resources, Funding acquisition, Conceptualization. J.W.: Writing—review & editing, Investigation, Funding acquisition, Conceptualization. G.Z.: Writing—review & editing, Investigation, Conceptualization. All authors have read and agreed to the published version of the manuscript.

Institutional Review Board Statement: Not applicable.

Data Availability Statement: The datasets generated during and/or analyzed during the current study are available from the corresponding author on reasonable request.

Conflicts of Interest: The authors declare no conflicts of interest.

References

1. Nuruzzaman, M.; Bahar, M.M.; Naidu, R. Diffuse soil pollution from agriculture: Impacts and remediation. *Sci. Total Environ.* **2025**, *962*, 178398. [CrossRef] [PubMed]

2. AbuQamar, S.F.; El-Saadony, M.T.; Saad, A.M.; Desoky, E.-S.M.; Elrys, A.S.; El-Mageed, T.A.A.; Semida, W.M.; Abdelkhalik, A.; Mosa, W.F.A.; Al Kafaas, S.S.; et al. Halotolerant plant growth-promoting rhizobacteria improve soil fertility and plant salinity tolerance for sustainable—A review. *Plant Stress* **2024**, *12*, 100482. [CrossRef]

3. Dey, S.; Haripavan, N.; Basha, S.R.; Babu, G.V. Removal of ammonia and nitrates from contaminated water by using solid waste bio-adsorbents. *Curr. Res. Chem. Biol.* **2021**, *1*, 100005. [CrossRef]

4. Bouselsal, B.; Satouh, A.; Egbueri, J.C.; Hashim, M.A.; Arafat, A.A.; Paramasivam, P.; Alzaed, A.; Hussein, E.E. Groundwater for drinking and sustainable agriculture and public health hazards of nitrate: Developmental and sustainability implications for an arid aquifer system. *Results Eng.* **2025**, *25*, 104160. [CrossRef]

5. Wei, Q.; Wei, Q.; Xu, J.; Liu, Y.; Wang, D.; Chen, S.; Qian, W.; He, M.; Chen, P.; Zhou, X.; et al. Nitrogen losses from soil as affected by water and fertilizer management under drip irrigation: Development, hotspots and future perspectives. *Agric. Water Manag.* **2024**, *296*, 108791. [CrossRef]

6. Zhao, S.; Wang, J.; Feng, S.; Xiao, Z.; Chen, C. Effects of ecohydrological interfaces on migrations and transformations of pollutants: A critical review. *Sci. Total Environ.* **2022**, *804*, 150140. [CrossRef]

7. Li, W.; Siddique, M.S.; Liu, M.; Graham, N.; Yu, W. The migration and microbiological degradation of dissolved organic matter in riparian soils. *Water Res.* **2022**, *224*, 119080. [CrossRef]

8. Harjung, A.; Schweichhart, J.; Rasch, G.; Griebler, C. Large-scale study on groundwater dissolved organic matter reveals a strong heterogeneity and a complex microbial footprint. *Sci. Total Environ.* **2023**, *854*, 158542. [CrossRef]

9. Singh, P.; Singh, M.K.; Beg, Y.R.; Nishad, G.R. A review on spectroscopic methods for determination of nitrite and nitrate in environmental samples. *Talanta* **2019**, *191*, 364–381. [CrossRef]

10. Ding, H.; Gao, H.; Zhu, M.; Yu, M.; Sun, Y.; Zheng, M.; Su, J.; Xi, B. Spectral and molecular insights into the characteristics of dissolved organic matter in nitrate-contaminated groundwater. *Environ. Pollut.* **2024**, *355*, 124202. [CrossRef]

11. Yeshno, E.; Dahan, O.; Bernstain, S.; Arnon, S. A novel analytical approach for the simultaneous measurement of nitrate and dissolved organic carbon in soil water. *Hydrol. Earth Syst. Sci.* **2021**, *25*, 2159–2168. [CrossRef]

12. Feng, X.; Wang, X.; Wei, Z.; Wu, M.; Ma, X.; Yan, X.; Shan, J. Depth weakens effects of long-term fertilization on dissolved organic matter chemodiversity in paddy soils. *Sci. Total Environ.* **2025**, *959*, 178237. [CrossRef] [PubMed]

13. Yeshno, E.; Arnon, S.; Dahan, O. Real-time monitoring of nitrate in soils as a key for optimization of agricultural productivity and prevention of groundwater pollution. *Hydrol. Earth Syst. Sci.* **2019**, *23*, 3997–4010. [CrossRef]

14. Sinfield, J.V.; Fagerman, D.; Colic, O. Evaluation of sensing technologies for on-the-go detection of macro-nutrients in cultivated soils. *Comput. Electron. Agric.* **2010**, *70*, 1–18. [CrossRef]

15. Lin, K.; Pei, J.; Li, P.; Ma, J.; Li, Q.; Yuan, D. Simultaneous determination of total dissolved nitrogen and total dissolved phosphorus in natural waters with an on-line UV and thermal digestion. *Talanta* **2018**, *185*, 419–426. [CrossRef]

16. Vullaganti, N.; Ram, B.G.; Sun, X. Precision agriculture technologies for soil site-specific nutrient management: A comprehensive review. *Artif. Intell. Agric.* **2025**, *15*, 147–161. [CrossRef]

17. Medel-Jiménez, F.; Krexner, T.; Gronauer, A.; Kral, I. Life cycle assessment of four different precision agriculture technologies and comparison with a conventional scheme. *J. Clean. Prod.* **2024**, *434*, 140198. [CrossRef]

18. Chen, R.; Chen, X.; Li, H.; Wang, J.; Guo, X. Evaluating soil water and nitrogen transport, nitrate leaching and soil nitrogen concentration uniformity under sprinkler irrigation and fertigation using numerical simulation. *J. Hydrol.* **2025**, *647*, 132345. [CrossRef]

19. Bogarin Cantero, B.C.; Zhang, Y.; Davidson, P.C. Electrolysis of HTL-AP for nutrient recovery by converting cyclic nitrogen to nitrate-N fertilizer. *Environ. Pollut.* **2024**, *363*, 125069. [CrossRef]

20. Kganyago, M.; Adjorlolo, C.; Mhangara, P.; Tsoeleng, L. Optical remote sensing of crop biophysical and biochemical parameters: An overview of advances in sensor technologies and machine learning algorithms for precision agriculture. *Comput. Electron. Agric.* **2024**, *218*, 108730. [CrossRef]

21. Raabe, J.M.; Kurtay, G.; Fontenot, A.; Greene, S.; Martignette, A.J.; Milbrandt, E.C.; Roberts, B.J.; Stauffer, B.A. Operation and integration of a commercially available nitrate sensor in Gulf of Mexico estuarine monitoring programs. *Environ. Technol. Innov.* **2024**, *35*, 103676. [CrossRef]

22. Zhuang, Y.; Wen, W.; Ruan, S.; Zhuang, F.; Xia, B.; Li, S.; Liu, H.; Du, Y.; Zhang, L. Real-time measurement of total nitrogen for agricultural runoff based on multiparameter sensors and intelligent algorithms. *Water Res.* **2022**, *210*, 117992. [CrossRef]

23. Venkatesh, J.; Partheeban, P.; Baskaran, A.; Krishnan, D.; Sridhar, M. Wireless sensor network technology and geospatial technology for groundwater quality monitoring. *J. Ind. Inf. Integr.* **2024**, *38*, 100569. [CrossRef]

24. Pal, A.; Dubey, S.K.; Goel, S.; Kalita, P.K. Portable sensors in precision agriculture: Assessing advances and challenges in soil nutrient determination. *TrAC Trends Anal. Chem.* **2024**, *180*, 117981. [CrossRef]

25. Ravikumar, S.; Vellingiri, G.; Sellaperumal, P.; Pandian, K.; Sivasankar, A.; Sangchul, H. Real-time nitrogen monitoring and management to augment N use efficiency and ecosystem sustainability—A review. *J. Hazard. Mater. Adv.* **2024**, *16*, 100466. [CrossRef]

26. Causse, J.; Thomas, O.; Jung, A.V.; Thomas, M.F. Direct DOC and nitrate determination in water using dual pathlength and second derivative UV spectrophotometry. *Water Res.* **2017**, *108*, 312–319. [CrossRef] [PubMed]

27. Liang, H.; Lv, H.; Batchelor, W.D.; Lian, X.; Wang, Z.; Lin, S.; Hu, K. Simulating nitrate and DON leaching to optimize water and N management practices for greenhouse vegetable production systems. *Agric. Water Manag.* **2020**, *241*, 106377. [CrossRef]

28. Fu, Y.; Li, W.; Li, H.; Huang, M. High-precision and on-line measurement of dissolved organic matter in Electro-Fenton process based on dual wavelength analysis with combination of fluorescence emission and ultraviolet absorption spectroscopy. *Anal. Chim. Acta* **2021**, *1181*, 338904. [CrossRef]

29. Arai, R.; Sakai, T.; Nishida, Y.; Inada, M. In situ temperature-compensated ultraviolet spectrophotometry to estimate nitrate and chloride concentrations in estuarine seawater with different salinity and composition. *J. Environ. Manag.* **2023**, *344*, 118689. [CrossRef]

30. Chu, W.; Yuan, L.; Huang, R.; Huang, D.; Zhuang, Y.; Ma, W.; Tian, M. Determination of glycyrrhizic acid as sweeteners by dual-wavelength overlapping resonance Rayleigh scattering. *Microchem. J.* **2024**, *202*, 110748. [CrossRef]

31. Miao, J.; Li, F.; Zhang, J.; Wei, B.; Ji, Y.; Yang, H. Optimization of Correction Factor of Soil Nitrate Nitrogen by Ultraviolet Spectrophotometry. *Acta Agric. Boreali-Sin.* **2019**, *34*, 204–212. [CrossRef]

32. Kafle, B.P. Chapter 5—Application of UV–VIS spectrophotometry for chemical analysis. In *Chemical Analysis and Material Characterization by Spectrophotometry*; Elsevier: Amsterdam, The Netherlands, 2020; pp. 79–145. [CrossRef]

33. Hu, H.; Tang, B.; Wan, H.; Sun, H.; Zhou, S.; Dai, J.; Chen, C.; Liu, S.; Guo, L.J. Boosted ultraviolet electroluminescence of InGaN/AlGaN quantum structures grown on high-index contrast patterned sapphire with silica array. *Nano Energy* **2020**, *69*, 104427. [CrossRef]

34. Mukunda, D.C.; Joshi, V.K.; Mahato, K.K. Light emitting diodes (LEDs) in fluorescence-based analytical applications: A review. *Appl. Spectrosc. Rev.* **2022**, *57*, 1–38. [CrossRef]

35. Natarajan, K.; Dave, S.; Bajaj, H.C.; Tayade, R.J. Enhanced photocatalytic degradation of nitrobenzene using MWCNT/β-ZnMoO$_4$ composites under UV light emitting diodes (LEDs). *Mater. Today Chem.* **2020**, *17*, 100331. [CrossRef]

36. Han, Y.-Z.; Tian, Y.-C.; Ji, W.-X.; Li, W.-B.; Xue, X.-F.; Dong, Y.-Q.; Guan, C.-Y.; Zhou, D.; Li, W.-T.; Lu, H.; et al. Development and application of the UVC LED-based spectrophotometer for high frequency online monitoring of nitrate concentration in municipal wastewater. *Sens. Actuators B Chem.* **2024**, *403*, 135178. [CrossRef]

37. Li, Y.; Dvořák, M.; Nesterenko, P.N.; Nuchtavorn, N.; Macka, M. High power deep UV-LEDs for analytical optical instrumentation. *Sens. Actuators B Chem.* **2018**, *255*, 1238–1243. [CrossRef]

38. Hamel, P.; Ding, N.; Cherqui, F.; Zhu, Q.; Walcker, N.; Bertrand-Krajewski, J.-L.; Champrasert, P.; Fletcher, T.D.; McCarthy, D.T.; Navratil, O.; et al. Low-cost monitoring systems for urban water management: Lessons from the field. *Water Res. X* **2024**, *22*, 100212. [CrossRef]

39. Dong, Q.-y.; Wen, H.-t.; Wang, P.; Song, C.; Lai, S.-y.; Yang, Z.-j.; Zhao, Y.-y.; Yan, M.-j. Health risk assessment of heavy metals in soils and crops in a mining area (Au-Ag-Cu-trona-oil et al.) of the Nanyang Basin, Henan Province, China. *China Geol.* **2023**, *6*, 567–579. [CrossRef]

40. Ran, S.; He, T.; Zhou, X.; Yin, D. Effects of fulvic acid and humic acid from different sources on Hg methylation in soil and accumulation in rice. *J. Environ. Sci.* **2022**, *119*, 93–105. [CrossRef]

41. Varma, K.; Jha, P.K.; Mukherjee, S.; Singhal, A.; Kumar, M. Provenances, preponderances, and distribution of humic acids and organic pollutants in hydro-geosphere: The co-existence, interaction and isotopic biomarkers in the riverine ecosystem. *J. Environ. Manag.* **2022**, *313*, 114996. [CrossRef]

42. Bagherifam, S.; Brown, T.C.; Bagherifam, S.; Baglieri, A. Sequential extraction of labile and recalcitrant fractions of soil organic matter: A case study focusing on antimony (Sb) in humic acids, fulvic acids and humin fractions of long-term aged contaminated soils. *Environ. Pollut.* **2023**, *327*, 121610. [CrossRef] [PubMed]

43. Kou, B.; Hui, K.; Miao, F.; He, Y.; Qu, C.; Yuan, Y.; Tan, W. Differential responses of the properties of soil humic acid and fulvic acid to nitrogen addition in the North China Plain. *Environ. Res.* **2022**, *214*, 113980. [CrossRef] [PubMed]

44. Frisch, M.; Trucks, G.; Schlegel, H.B.; Scuseria, G.E.; Robb, M.; Cheeseman, J.R.; Scalmani, G.; Barone, V.; Petersson, G.A.; Nakatsuji, H.; et al. *Gaussian 16 Revision A.03*; Gaussian: Wallingford, CT, USA, 2016.

45. Lu, T.; Chen, F.W. Multiwfn: A multifunctional wavefunction analyzer. *J. Comput. Chem.* **2012**, *33*, 580–592. [CrossRef]

46. Humphrey, W.; Dalke, A.; Schulten, K. VMD: Visual molecular dynamics. *J. Mol. Graph.* **1996**, *14*, 33–38. [CrossRef]

47. Wenzel, T.J. Douglas A. Skoog, Donald M. West, F. James Holler, and Stanley R. Crouch: Fundamentals of analytical chemistry, 9th ed., international ed. *Anal. Bioanal. Chem.* **2013**, *405*, 7903–7904. [CrossRef]

48. Cai, M.H.; Tian, Y.C.; Li, A.M.; Li, Y.; Han, Y.Z.; Ji, W.X.; Zhou, Q.; Li, J.; Li, W.T. Unraveling the evolution of dissolved organic matter in full-scale A/A/O wastewater treatment process using size exclusion chromatography with PARAFAC and nonnegative matrix factorization analysis. *Water Res.* **2023**, *235*, 119879. [CrossRef] [PubMed]

49. Silva, M.F.; Bermejo de Lima, L.; de Camargo, C.; Telles Benatti, C. Usability of simplified UV–Vis spectrophotometric methods for the determination of nitrate in the presence of organic matter and chloride as interfering factors. *Water Pract. Technol.* **2024**, *19*, 1061–1070. [CrossRef]

50. Huebsch, M.; Grimmeisen, F.; Zemann, M.; Fenton, O.; Richards, K.G.; Jordan, P.; Sawarieh, A.; Blum, P.; Goldscheider, N. Technical Note: Field experiences using UV/VIS sensors for high-resolution monitoring of nitrate in groundwater. *Hydrol. Earth Syst. Sci.* **2015**, *19*, 1589–1598. [CrossRef]

51. Li, Y.; Nesterenko, P.N.; Paull, B.; Stanley, R.; Macka, M. Performance of a New 235 nm UV-LED-Based On-Capillary Photometric Detector. *Anal. Chem.* **2016**, *88*, 12116–12121. [CrossRef]

52. Wang, F.-X.; Chen, Y.; Liang, Y.-M.; Yang, M.; Kang, C. Interference-free quantitation of aromatic amino acids in two complex systems by three-way calibration with ultraviolet–visible spectrophotometer: Exploration of trilinear decomposition of spectrum-pH data. *Spectrochim. Acta Part A Mol. Biomol. Spectrosc.* **2023**, *290*, 122293. [CrossRef]

53. Qiang, L.; Ancheng, L.; Chisheng, Y.; Kaiying, C.; Hamid, Y.; Zhiwei, L.; Yunlong, W.; Wenchen, Y. Insights into the role of endogenous humic acid on antibiotics bioadsorption process in wastewater: Mechanisms and potential implications. *J. Water Process Eng.* **2024**, *64*, 105606. [CrossRef]

54. Mörschbächer, A.P.; Dullius, A.; Dullius, C.H.; Bandt, C.R.; Kuhn, D.; Brietzke, D.T.; Malmann Kuffel, F.J.; Etgeton, H.P.; Altmayer, T.; Gonçalves, T.E.; et al. Validation of an analytical method for the quantitative determination of selenium in bacterial biomass by ultraviolet–visible spectrophotometry. *Food Chem.* **2018**, *255*, 182–186. [CrossRef] [PubMed]

55. Uusheimo, S.; Tulonen, T.; Arvola, L.; Arola, H.; Linjama, J.; Huttula, T. Organic carbon causes interference with nitrate and nitrite measurements by UV/Vis spectrometers: The importance of local calibration. *Environ. Monit. Assess.* **2017**, *189*, 357. [CrossRef] [PubMed]

56. *GB/T 32737-2016*; Determination of Nitrate Nitrogen in Soil—Ultraviolet Spectrophotometry Method. Standardization Administration of China (SAC): Beijing, China, 2016.

57. Dong, J.; Tang, J.; Wu, G.; Xin, Y.; Li, R.; Li, Y. Effective correction of dissolved organic carbon interference in nitrate detection using ultraviolet spectroscopy combined with the equivalent concentration offset method. *RSC Adv.* **2024**, *14*, 5370–5379. [CrossRef]

58. Magdoff, F.; van Es, H. *Amount of Organic Matter in Soils. Building Soils for Better Crops*, 4th ed.; SARE Outreach: College Park, MD, USA, 2021; p. 410.

59. Tian, S.; Yao, S.; Zhu, S.; Li, P.; Zhang, T.; Su, X.; Huang, R.; Yin, Y.; Lv, J.; Jiang, T.; et al. Evaluating soil dissolved organic matter as a proxy for soil organic matter properties across diverse ecosystems. *Soil Biol. Biochem.* **2025**, *204*, 109752. [CrossRef]

60. Mitrakas, M.; Tsitouridou, R.; Keramidas, V. Interference of Humic Substances in the Spectrophotometric Determination of Bromate by Phenothiazines in Natural Waters. *Int. J. Environ. Anal. Chem.* **2000**, *78*, 343–351. [CrossRef]

61. Edwards, A.C.; Hooda, P.S.; Cook, Y. Determination of Nitrate in Water Containing Dissolved Organic Carbon by Ultraviolet Spectroscopy. *Int. J. Environ. Anal. Chem.* **2001**, *80*, 49–59. [CrossRef]

62. Moo, Y.C.; Matjafri, M.Z.; Lim, H.S.; Tan, C.H. New development of optical fibre sensor for determination of nitrate and nitrite in water. *Optik* **2016**, *127*, 1312–1319. [CrossRef]

63. Lal, K.; Jaywant, S.A.; Arif, K.M. Electrochemical and Optical Sensors for Real-Time Detection of Nitrate in Water. *Sensors* **2023**, *23*, 7099. [CrossRef]

64. De Notaris, C.; Rasmussen, J.; Sørensen, P.; Olesen, J.E. Nitrogen leaching: A crop rotation perspective on the effect of N surplus, field management and use of catch crops. *Agric. Ecosyst. Environ.* **2018**, *255*, 1–11. [CrossRef]

65. Cui, J.; Zhang, X.; Reis, S.; Wang, C.; Wang, S.; He, P.; Chen, H.; van Grinsven, H.J.M.; Gu, B. Nitrogen cycles in global croplands altered by elevated CO_2. *Nat. Sustain.* **2023**, *6*, 1166–1176. [CrossRef]

66. Wen, T.; Yu, G.-H.; Hong, W.-D.; Yuan, J.; Niu, G.-Q.; Xie, P.-H.; Sun, F.-S.; Guo, L.-D.; Kuzyakov, Y.; Shen, Q.-R. Root exudate chemistry affects soil carbon mobilization via microbial community reassembly. *Fundam. Res.* **2022**, *2*, 697–707. [CrossRef] [PubMed]

67. Kareem, A.; Farooqi, Z.U.R.; Kalsom, A.; Mohy-Ud-Din, W.; Hussain, M.M.; Raza, M.; Khursheed, M.M. Organic Farming for Sustainable Soil Use, Management, Food Production and Climate Change Mitigation. In *Sustainable Agriculture: Technical Progressions and Transitions*; Bandh, S.A., Ed.; Springer International Publishing: Cham, Switzerland, 2022; pp. 39–59.

68. Li, X.; Zhu, W.; Xu, F.; Du, J.; Tian, X.; Shi, J.; Wei, G. Organic amendments affect soil organic carbon sequestration and fractions in fields with long-term contrasting nitrogen applications. *Agric. Ecosyst. Environ.* **2021**, *322*, 107643. [CrossRef]